Journal of Mathematical Biology (2021) 82:60
https://doi.org/10.1007/s00285-021-01608-z

Mathematical Biology

A systematic search for switch-like behavior in type II toxin–antitoxin systems

Cody E. FitzGerald[1] · James P. Keener[1]

Received: 1 February 2020 / Revised: 8 February 2021 / Accepted: 15 April 2021 / Published online: 15 May 2021

Abstract

Bistable switch-like behavior is a ubiquitous feature of gene regulatory networks with decision-making capabilities. Type II toxin-antitoxin (TA) systems are hypothesized to facilitate a bistable switch in toxin concentration that influences the dormancy transition in persister cells. However, a series of recent retractions has raised fundamental questions concerning the exact mechanism of toxin propagation in persister cells and the relationship between type II TA systems and cellular dormancy. Through a careful modeling search, we identify how sp: bistablilty can emerge in type II TA systems by systematically modifying a basic model for the RelBE system with other common biological mechanisms. Our systematic search uncovers a new combination of mechanisms influencing bistability in type II TA systems and explores how toxin bistability emerges through synergistic interactions between paired type II TA systems. Our analysis also illustrates how Descartes' rule of signs and the resultant can be used as a powerful delineator of bistability in mathematical systems regardless of application.

Keywords Toxin–antitoxin systems · Type II toxin–antitoxin systems · Bistability · Switches · Mathematical modeling · Resultant · Resultant analysis · Synergy · Cross-talk

Mathematics Subject Classification 92C42 · 34C42

✉ Cody E. FitzGerald
cfitz@math.utah.edu

[1] Department of Mathematics, University of Utah, 155 South 1400 East, Salt Lake City, UT 84112, USA

1 Introduction

Toxin–antitoxin (TA) systems exist in many species of bacteria, some pathogenic. TA systems have been classified into six different types. Of the six types, type II TA systems are the most well-understood, and many examples, such as the RelBE system, have been identified. For a general review of TA systems, see Harms et al. (2018) and Unterholzner et al. (2013). Type II TA systems have two components: the toxin and the antitoxin. The direct neutralization of toxin by the antitoxin through complex formation is the defining characteristic of type II TA systems. The toxin and antitoxin genes are found in an operon, often called the TA operon. The genes are transcribed together, then translated into active protein forms. Operon transcription is autoregulated by the protein form of the antitoxin and the complex (Bukowski et al. 2011). The toxin and antitoxin serve reciprocal functions in the cell: the toxin interferes with intracellular processes, such as mRNA translation, while the antitoxin neutralizes the toxin through complex formation.

Bistable switch-like behavior is a common feature of gene regulatory networks with decision-making capabilities. Gene regulatory networks exhibiting bistability are widespread across cell biology and have been modeled extensively. Recent papers have modeled gene regulatory and signalling networks that govern the regulation of the p53 pathway, the neuroscience of memory, and cell fate in the *Drosophila* eye (Graham et al. 2010; Puszyński et al. 2008; Smolen et al. 2019). If type II TA systems are bistable, two distinct states would exist: one with a high toxin concentration and the other with a low toxin concentration, corresponding to a disruptive and normal state, respectively. The general biology of type II TA systems influencing such a switch between the high and low toxin state are reasonably well understood. Generated imbalances in toxin concentrations disrupt basic intracellular processes such as translation. These imbalances in toxin and antitoxin concentrations arise through asymmetries in the system in the form of degradational differences between proteins and transcriptional regulation. The antitoxin is a relatively unstable protein compared to the toxin and is degraded by proteases such as Lon and Clp. The antitoxin protein and some complexes are known to repress the TA operon, while the toxin acts as an operon activator or derepressor. This specific operon activation/repression scheme in which stoichiometric changes in toxin, antitoxin, and complex concentrations lead to different transcriptional behavior is known as conditional cooperativity (Afif et al. 2001; Garcia-Pino et al. 2010; Overgaard et al. 2008).

While some biology of type II TA systems is reasonably well-understood, the exact mechanistic details that could facilitate a switch between the high and low toxin state remain unclear. Notably, several recent papers linking type II TA systems to persister cells were retracted, causing the degree to which type II TA systems influence the dormancy transitions of persister cells to be called into question (Germain et al. 2019; Maisonneuve et al. 2018a, b). The retraction has caused confusion regarding the biology of switch-like behavior in type II TA systems. Earlier studies are now being redone and conflicting results have been found (Harms et al. 2017; Goormaghtigh et al. 2018; Fraikin et al. 2019). Additionally, previous modeling attempts have not taken a systematic approach to identify biologically feasible genetic architectures which control the switch between the disruptive and normal state (Cataudella et al.

2013; Lou et al. 2008). The idea that type II toxin–antitoxin systems may exhibit graded rather than switch-like responses was recently examined in an opinion piece (Ramisetty 2020). For these reasons, a systematic evaluation of which mechanisms control the emergence of bistability in type II TA systems is warranted.

In this paper, we provide that systematic study. We first prove that a basic model of the RelBE system cannot be bistable for any positive parameter values. Next, we modify the model with additional mechanisms to systematically find a biologically-relevant type II TA system model for which switch-like bistability can occur. We consider the following list of biologically reasonable mechanisms in the search for bistability:

1. Antitoxin-mediated degradation of mRNA (known feature of type I TA systems) and other mRNA degradation variants.
2. Decoupling of the antitoxin and toxin production rates (assumption used in previous models, for example see Cataudella et al. 2013).
3. Toxin-dependent degradation of the antitoxin (hypothesized indirect mechanism of type II TA systems from the retracted system, for example, see Germain et al. 2019).
4. Toxin-dependent operon activation or derepression (a common feature of type II TA systems).
5. Additional operon repression by the antitoxin or complexes (a common feature of type II TA systems).
6. A combination of the above mechanisms.

In each case, we either prove that bistability cannot occur or demonstrate a parameter regime for which bistable behavior exists. This analysis not only demonstrates how Descartes' rule of signs and resultant analysis can be used together as a potent delineator in the search for bistable behavior across many mathematical systems, but also provides new biological insight into type II TA systems. In particular, we propose a new theoretical model of a type II TA system in which toxin-dependent operon derepression in tandem with other mechanisms controls the emergence of switch-like behavior and show how cross-talk or synergy between paired type II TA systems can drive the emergence of toxin bistability.

2 Results

2.1 A mathematical model of the RelBE system

We begin by analyzing a basic model of the RelBE system. The model includes two operon states (ON and OFF); mRNA; antitoxin; toxin; and two complexes, C_1 and C_2. Figure 1 is a reaction diagram for the RelBE model. The operon is pictured in blue and maroon, representing the antitoxin and toxin gene, respectively. When the operon is derepressed, transcription of both antitoxin and toxin mRNA occurs, which are then translated into the two active protein forms. The active protein form of the antitoxin and toxin are represented by the blue circle and the maroon triangle, respectively. In this model, mRNA, the toxin protein, and the antitoxin protein are assumed to degrade.

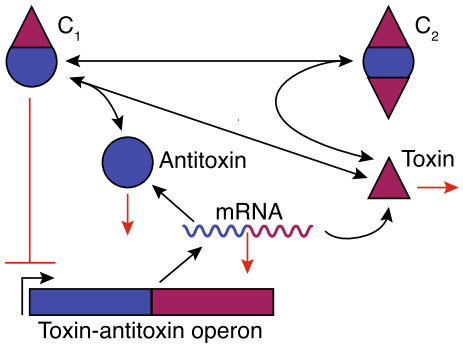

Fig. 1 Reaction diagram for the basic RelBE model. The model includes two operon states (ON and OFF); mRNA; antitoxin; toxin; and two complexes, C_1 and C_2. The operon is pictured in blue and maroon, representing the antitoxin and toxin gene, respectively. When the operon is derepressed, transcription of both antitoxin and toxin mRNA occurs, which are then translated into the two active protein forms. The active protein form of the antitoxin and toxin are represented by the blue circle and the maroon triangle, respectively. In this model, mRNA, the toxin protein, and the antitoxin protein are assumed to degrade. The first complex, C_1, is comprised of an antitoxin and toxin protein. We assume that C_1 can dissociate, repress the operon, but does not degrade. C_2, the second complex, is formed through the association of C_1 and an additional toxin monomer. C_2 has no role in operon repression, is assumed to dissociate, but not degrade. In the reaction diagram, black arrows represent physical transitions, and red arrows represent degradation or operon repression

The first complex, C_1, is comprised of an antitoxin and toxin protein. We assume that C_1 can dissociate, repress the operon, but does not degrade. C_2, the second complex, is formed through the association of C_1 and an additional toxin monomer. C_2 has no role in operon repression, is assumed to dissociate, but not degrade. In the reaction diagram, black arrows represent physical transitions, and red arrows represent degradation or operon repression.

The dimensional differential equation model for this system has the following representation:

$$\frac{dO_p}{dt} = k(1 - O_p) - k_- C_1 O_p \tag{1}$$

$$\frac{dM}{dt} = k_m O_p - k_{-m} M \tag{2}$$

$$\frac{dA}{dt} = k_{ta} M - k_{-a} A - \alpha A T + \alpha_- C_1 \tag{3}$$

$$\frac{dT}{dt} = k_{ta} M - k_{-t} T - \alpha A T + \alpha_- C_1 - \beta C_1 T + \beta_- C_2 \tag{4}$$

$$\frac{dC_1}{dt} = \alpha A T - \alpha_- C_1 - \beta C_1 T + \beta_- C_2 \tag{5}$$

$$\frac{dC_2}{dt} = \beta C_1 T - \beta_- C_2, \tag{6}$$

where O_p represents the probability the operon is in the ON state (O_r represents the probability the operon is in the OFF state and $O_p + O_r = 1$), and M, A, T, C_1, C_2 represent concentrations of mRNA, antitoxin, toxin, the first complex, and the second complex, respectively.

Claim 1 The basic RelBE model described by Eqs. (1)–(6) cannot exhibit bistability in toxin concentration.

Proof The steady-state equations for the system (1)–(6) can be reduced to a single polynomial equation for the variable T, of the form:

$$n_1(T) = s_3 T^3 + s_1 T - s_0 = 0,$$

where s_3, s_1, and s_0 are combinations of model parameters and are non-negative for all non-negative parameter values. The coefficients s_3, s_1, and s_0 are defined as:

$$\begin{aligned} s_3 &= k_{-t}^2 k_{-m} \alpha k_- \\ s_1 &= \alpha_- k k_{-a} k_{-m} k_{-t} \\ s_0 &= \alpha_- k k_m k_{-a} k_{ta}. \end{aligned}$$

The existence of three positive roots for some positive parameter regime is a necessary condition for finding biologically relevant bistability. By Descartes' rule of signs, $n_1(T)$ has only one positive root regardless of the parameter regime. Therefore, the RelBE model as formulated cannot exhibit bistability in toxin concentration for any parameter regime. □

2.2 Modeling assumptions

When evaluating the different type II TA system-like models for bistability, we make four main assumptions. The first is that the toxin and antitoxin genes are in the same operon. There is no evidence to suggest that the toxin and antitoxin genes are found separately in the genome for most known type II TA systems. The second assumption is that the first complex, a heterodimer of toxin and antitoxin, represses the operon. The first complex is the strongest known repressor of the operon. The antitoxin is a weaker operon repressor, and for this reason, we ignore it in some of the models we consider. In models where we include both the first complex and antitoxin as operon repressors, the binding rate of the first complex is higher than the binding rate of the antitoxin to reflect the relative strength of the first complex as an operon repressor. The third assumption is that the natural degradation rate of the antitoxin is higher than the natural degradation rate of the toxin to reflect the unstable nature of the antitoxin. Lastly, we do not include antitoxin dimerization for model simplicity.

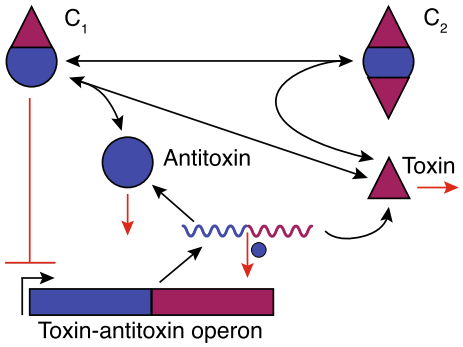

Fig. 2 Reaction diagram for the antitoxin-mediated degradation of mRNA model. The model includes two operon states (ON and OFF); mRNA; antitoxin; toxin; and two complexes, C_1 and C_2. The operon is pictured in blue and maroon, representing the antitoxin and toxin gene, respectively. When the operon is derepressed, transcription of both antitoxin and toxin mRNA occurs, which are then translated into the two active protein forms. The active protein form of the antitoxin and toxin are represented by the blue circle and the maroon triangle, respectively. In this model, mRNA, the toxin protein, and the antitoxin protein are assumed to degrade. The first complex, C_1, is comprised of an antitoxin and toxin protein. We assume that C_1 can dissociate, repress the operon, but does not degrade. C_2, the second complex, is formed through the association of C_1 and an additional toxin monomer. C_2 has no role in operon repression, is assumed to dissociate, but not degrade. In the reaction diagram, black arrows represent physical transitions, and red arrows represent degradation or operon repression. The new feature of this model is the antitoxin-mediated degradation of mRNA (color figure online)

2.3 Models that are not bistable with proof

2.3.1 Mediated degradation of mRNA RelBE model

Next, we modify the basic RelBE model to include antitoxin-mediated degradation of mRNA, a mechanism observed in type I TA systems. We also consider toxin and complex-mediated degradation of mRNA model variants. Figure 2 is a reaction diagram for the antitoxin-mediated degradation of mRNA model. In the reaction diagram, the new interaction is denoted by the antitoxin appearing next to the red mRNA degradation arrow. All assumptions from the original RelBE model carry over. The dimensional differential equation model has the following representation:

$$\frac{dO_p}{dt} = k(1 - O_p) - k_- C_1 O_p \tag{7}$$

$$\frac{dM}{dt} = k_m O_p - k_{-m} M \boxed{-k_{-m_2} M A} \tag{8}$$

$$\frac{dA}{dt} = k_{ta} M - k_{-a} A - \alpha A T + \alpha_- C_1 \tag{9}$$

$$\frac{dT}{dt} = k_{ta} M - k_{-t} T - \alpha A T + \alpha_- C_1 - \beta C_1 T + \beta_- C_2 \tag{10}$$

$$\frac{dC_1}{dt} = \alpha AT - \alpha_- C_1 - \beta C_1 T + \beta_- C_2 \tag{11}$$

$$\frac{dC_2}{dt} = \beta C_1 T - \beta_- C_2, \tag{12}$$

where all variables retain their meaning from the basic RelBE model, and the new term is shown outlined by a dashed box.

Claim 2 The modification of the basic RelBE model described by Eqs. (7)–(12) cannot exhibit bistability in toxin concentration.

Proof The steady-state equations for the system (7)–(12) can be reduced to a single polynomial equation in A, which has the form:

$$n_1(A) = s_4 A^4 + s_3 A^3 + s_2 A^2 + s_1 A - s_0 = 0.$$

where s_4, s_3, s_2, s_1, and s_0 are combinations of model parameters and are non-negative for all non-negative parameter values. Using the same argument based on Descartes' rule of sign presented in Sect. 2.1, this model cannot exhibit bistability in toxin concentration for any positive parameter regime. The same argument holds for model variants where either complex or the toxin mediates mRNA degradation. However, the model variant in which C_1 mediates the degradation of mRNA requires the use of the resultant[1] to prove the system cannot exhibit bistability. The full calculation is done in detail in the Appendix. □

2.3.2 RelBE model with uncoupled translation rates

Next, we modify the basic RelBE model by uncoupling the translation rates. Figure 3 is a reaction diagram for the RelBE model with uncoupled translation rates. In the reaction diagram, the antitoxin and toxin translation rates are represented by blue and maroon arrows, respectively. All assumptions from the original RelBE model carry over. The dimensional differential equation model has the following representation:

$$\frac{dO_p}{dt} = k(1 - O_p) - k_- C_1 O_p \tag{13}$$

$$\frac{dM}{dt} = k_m O_p - k_{-m} M \tag{14}$$

$$\frac{dA}{dt} = \boxed{k_{ta_1}} M - k_{-a} A - \alpha AT + \alpha_- C_1 \tag{15}$$

[1] The resultant is defined as the determinant of the Sylvester Matrix, which is built from the coefficients of two polynomials of any degree. The resultant is proportional to the product of the difference of the two polynomial's roots. In particular, the resultant is zero if and only if the two polynomials share a common root. This fact can be exploited to search for double roots of a polynomial and reduce a system of n polynomials in n unknowns to a single polynomial in one variable. The resultant is a useful, but little-known tool for nonlinear ODE model analysis. Additionally the resultant can be easily computed using a computer algebra system like Maple.

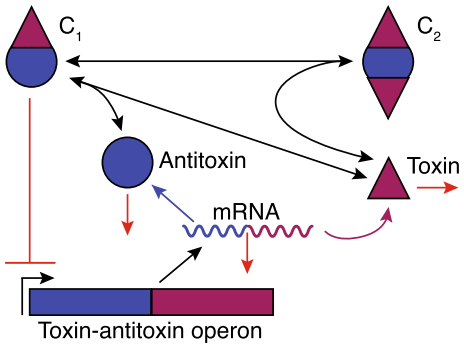

Fig. 3 Reaction diagram for the RelBE model with uncoupled translation rates. The model includes two operon states (ON and OFF); mRNA; antitoxin; toxin; and two complexes, C_1 and C_2. The operon is pictured in blue and maroon, representing the antitoxin and toxin gene, respectively. When the operon is derepressed, transcription of both antitoxin and toxin mRNA occurs, which are then translated into the two active protein forms. The active protein form of the antitoxin and toxin are represented by the blue circle and the maroon triangle, respectively. In this model, mRNA, the toxin protein, and the antitoxin protein are assumed to degrade. The first complex, C_1, is comprised of an antitoxin and toxin protein. We assume that C_1 can dissociate, repress the operon, but does not degrade. C_2, the second complex, is formed through the association of C_1 and an additional toxin monomer. C_2 has no role in operon repression, is assumed to dissociate, but not degrade. In the reaction diagram, black arrows represent physical transitions, and red arrows represent degradation or operon repression. The new feature of this model is the uncoupled antitoxin and toxin translation rates (color figure online)

$$\frac{dT}{dt} = \boxed{k_{ta_2}} M - k_{-t}T - \alpha AT + \alpha_- C_1 - \beta C_1 T + \beta_- C_2 \tag{16}$$

$$\frac{dC_1}{dt} = \alpha AT - \alpha_- C_1 - \beta C_1 T + \beta_- C_2 \tag{17}$$

$$\frac{dC_2}{dt} = \beta C_1 T - \beta_- C_2 \tag{18}$$

where all variables retain their meaning from the basic RelBE model and the new terms are shown outlined by dashed boxes.

Claim 3 The modification of the basic RelBE model described by Eqs. (13)–(18) cannot exhibit bistability in toxin concentration.

Proof The steady-state equations for the system (13)–(18) can be reduced to a single cubic polynomial equation in T with the following form:

$$s_3 T^3 + s_1 T - s_0 = 0.$$

We can use the same argument as in Sect. 2.1 to show conclusively that this model cannot exhibit bistability in toxin concentration for any positive parameter regime. □

2.3.3 RelBE model with toxin-dependent degradation of the antitoxin

We now consider a modification of the basic RelBE model that includes quadratic toxin-dependent degradation of the antitoxin. Antitoxin is degraded by the protein Lon or Clp in many type II TA systems. The assumption here is that the toxin indirectly aids in Clp or Lon-dependent degradation, but for simplicity, we insert a direct degradation effect by the toxin on the antitoxin into the model. It should be noted that the linear toxin-dependent degradation of the antitoxin variant of the model cannot be bistable. This can be proved using the argument from Sect. 2.1. We do not include higher order toxin-dependent antitoxin degradation terms because there is not a clear biological rationale to do so.

Figure 4 is a reaction diagram for this model. In the reaction diagram, the quadratic toxin-mediated antitoxin degradation is represented by the toxin dimer near the antitoxin degradation arrow. All assumptions from the original RelBE model carry over. The dimensional differential equation model has the following representation:

$$\frac{dO_p}{dt} = k(1 - O_p) - k_- C_1 O_p \tag{19}$$

$$\frac{dM}{dt} = k_m O_p - k_{-m} M \tag{20}$$

$$\frac{dA}{dt} = k_{ta} M - k_{-a} A - \alpha A T + \alpha_- C_1 \boxed{-k_s A T^2} \tag{21}$$

$$\frac{dT}{dt} = k_{ta} M - k_{-t} T - \alpha A T + \alpha_- C_1 - \beta C_1 T + \beta_- C_2 \tag{22}$$

$$\frac{dC_1}{dt} = \alpha A T - \alpha_- C_1 - \beta C_1 T + \beta_- C_2 \tag{23}$$

$$\frac{dC_2}{dt} = \beta C_1 T - \beta_- C_2, \tag{24}$$

where all variables retain their meaning from the basic RelBE model, and the new term is outlined by a dashed box.

Claim 4 The modification of the basic RelBE model, described by Eqs. (19)–(24) cannot exhibit bistability in toxin concentration.

Proof The steady-state equations for the system (19)–(24) can be reduced to a single cubic polynomial, which has the form:

$$n_1(T) = s_3 T^3 - s_2 T^2 + s_1 T - s_0 = 0,$$

where s_3,s_2,s_1, and s_0 are combinations of model parameters and are non-negative for all non-negative parameter values.

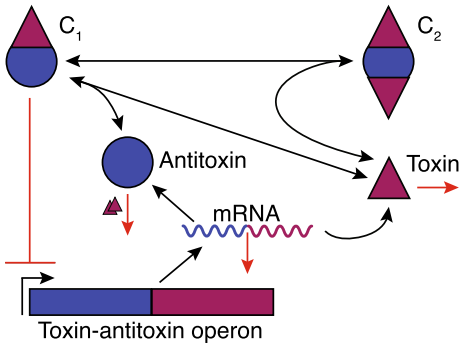

Fig. 4 Reaction diagram for the RelBE model with toxin-mediated degradation of the antitoxin. The model includes two operon states (ON and OFF); mRNA; antitoxin; toxin; and two complexes, C_1 and C_2. The operon is pictured in blue and maroon, representing the antitoxin and toxin gene, respectively. When the operon is derepressed, transcription of both antitoxin and toxin mRNA occurs, which are then translated into the two active protein forms. The active protein form of the antitoxin and toxin are represented by the blue circle and the maroon triangle, respectively. In this model, mRNA, the toxin protein, and the antitoxin protein are assumed to degrade. The first complex, C_1, is comprised of an antitoxin and toxin protein. We assume that C_1 can dissociate, repress the operon, but does not degrade. C_2, the second complex, is formed through the association of C_1 and an additional toxin monomer. C_2 has no role in operon repression, is assumed to dissociate, but not degrade. In the reaction diagram, black arrows represent physical transitions, and red arrows represent degradation or operon repression. The new feature of this model is the toxin-mediated degradation of the antitoxin (color figure online)

The existence of three positive roots for some positive parameter regime is a necessary condition for finding biologically relevant bistability. By Descartes' rule of signs, $n_1(T)$ can have either one or three positive roots. To find bistability, we need to find a parameter regime for which there are three positive roots. To find switch-like bistability (or a region of instability more generally), the steady state equation (in this case the cubic polynomial, n_1) must transition from having a single positive root, to three distinct positive roots (one unstable and two stable), to a different single stable root as a function of a model parameter. Transitions between one and three roots occur when $n_1(T)$ and $n_1'(T)$ are both equal to zero. The resultant of $n_1(T)$ and $n_1'(T)$ with respect to T identifies simultaneous zeroes of the two polynomials. In this case, the resultant is a strictly positive polynomial of model parameters. Therefore, for any positive parameter regime one cannot find a double root of $n_1(T)$. This rules out the possibility of a switch from one to three roots for this model. Plugging in an arbitrary parameter set (all model parameters equal to 1) leads to

$$\text{Resultant}(n_1(T), n_1'(T))(T) = 2T^3 - T^2 + T - 1,$$

which is a monotone increasing function of T and so has only one positive root.Thus, this system has only one positive root for all positive parameter regimes and is not bistable. Therefore, the RelBE model with quadratic toxin-dependent degradation of the antitoxin cannot exhibit bistability in toxin concentration for any positive parameter regime. □

2.3.4 RelBE model with toxin-dependent operon activation

We now consider a modification of the basic RelBE model that includes both monomeric and dimeric-toxin-dependent activation of the operon. The analysis is shown only for the dimer case. Other bistable systems, such as the SOS response, include activation of specific genes. During the SOS response, RecA binds to single-stranded DNA and cleaves LexA off the promoter site, activating transcription of select DNA damage genes. We consider a similar mechanism here in which the toxin pulls the first complex off the repressor site, activating the TA operon. Figure 5 is a reaction diagram for this model. In the reaction diagram, toxin-activation of the operon is represented by the green arrow and toxin next to the operon. All assumptions from the original RelBE model carry over. The dimensional differential equation model has the following representation:

$$\frac{dO_p}{dt} = \boxed{kT^2}(1 - O_p) - k_- C_1 O_p \tag{25}$$

$$\frac{dM}{dt} = k_m O_p - k_{-m} M \tag{26}$$

$$\frac{dA}{dt} = k_{ta} M - k_{-a} A - \alpha A T + \alpha_- C_1 \tag{27}$$

$$\frac{dT}{dt} = k_{ta} M - k_{-t} T - \alpha A T + \alpha_- C_1 - \beta C_1 T + \beta_- C_2 \tag{28}$$

$$\frac{dC_1}{dt} = \alpha A T - \alpha_- C_1 - \beta C_1 T + \beta_- C_2 \tag{29}$$

$$\frac{dC_2}{dt} = \beta C_1 T - \beta_- C_2, \tag{30}$$

where all variables retain their meaning from the basic RelBE model, and the new term is outlined by a dashed box.

Claim 5 The modification of the basic RelBE model described by Eqs. (25)–(30) cannot exhibit bistability in toxin concentration.

Proof The steady-state equations for the system (25)–(30) can be reduced to a single polynomial in T, which has the form:

$$n_1(T) = s_1 T - s_0 = 0,$$

where s_1 and s_0 are positive combinations of model parameters. Clearly, this model has a single unique positive solution and therefore cannot exhibit switch-like bistability in toxin concentration for any positive parameter regime. This shows that dimerized toxin has no influence on the emergence of switch-like bistability when acting alone

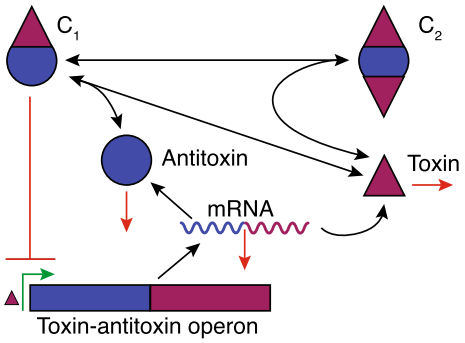

Fig. 5 Reaction diagram for the RelBE model with toxin-dependent activation of the operon. The model includes two operon states (ON and OFF); mRNA; antitoxin; toxin; and two complexes, C_1 and C_2. The operon is pictured in blue and maroon, representing the antitoxin and toxin gene, respectively. When the operon is derepressed, transcription of both antitoxin and toxin mRNA occurs, which are then translated into the two active protein forms. The active protein form of the antitoxin and toxin are represented by the blue circle and the maroon triangle, respectively. In this model, mRNA, the toxin protein, and the antitoxin protein are assumed to degrade. The first complex, C_1, is comprised of an antitoxin and toxin protein. We assume that C_1 can dissociate, repress the operon, but does not degrade. C_2, the second complex, is formed through the association of C_1 and an additional toxin monomer. C_2 has no role in operon repression, is assumed to dissociate, but not degrade. In the reaction diagram, black arrows represent physical transitions, and red arrows represent degradation or operon repression. The new feature of this model is the toxin-mediated operon activation (color figure online)

as an operon activator. The same result can also be shown for a toxin monomeric activator. We did not consider higher order toxin structures because there is no clear biological rationale to do so.

We could also consider a similar model formulation in which the concentration of toxin does not increase the probability the operon is in the ON state, but rather decreases the probability the operon is in the OFF state. The operon equation in the latter case has the following form:

$$\frac{dO_p}{dt} = k(1 - O_p) - k_{-1}\frac{C_1 O_p}{k_{-3} + k_{-4}T^2}.$$

It can be shown that a model of this form also cannot exhibit bistable switch-like behavior in the monomeric and dimeric cases. Again, we do not include higher order toxin terms in the saturating function because there is not a clear biological rationale for such terms. □

2.3.5 RelBE model with additional operon repression

We now consider a modification of the basic RelBE model that includes additional operon repression from the antitoxin, a relatively weaker operon repressor. Figure 6 is the reaction diagram for this model. The modification is shown as a red line from antitoxin to the operon. All assumptions from the original RelBE model carry over. The dimensional differential equation model has the following representation:

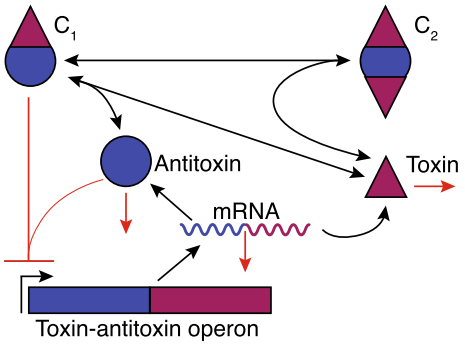

Fig. 6 Reaction diagram for the RelBE model with antitoxin-mediated operon repression. The model includes two operon states (ON and OFF); mRNA; antitoxin; toxin; and two complexes, C_1 and C_2. The operon is pictured in blue and maroon, representing the antitoxin and toxin gene, respectively. When the operon is derepressed, transcription of both antitoxin and toxin mRNA occurs, which are then translated into the two active protein forms. The active protein form of the antitoxin and toxin are represented by the blue circle and the maroon triangle, respectively. In this model, mRNA, the toxin protein, and the antitoxin protein are assumed to degrade. The first complex, C_1, is comprised of an antitoxin and toxin protein. We assume that C_1 can dissociate, repress the operon, but does not degrade. C_2, the second complex, is formed through the association of C_1 and an additional toxin monomer. C_2 has no role in operon repression, is assumed to dissociate, but not degrade. In the reaction diagram, black arrows represent physical transitions, and red arrows represent degradation or operon repression. The new feature of this model is the antitoxin-mediated repression of the operon, which is represented by the red arrow from the antitoxin to the operon (colour figure online)

$$\frac{dO_p}{dt} = k(1 - O_p) - k_- C_1 O_p \boxed{-k_{-_2} A O_p} \tag{31}$$

$$\frac{dM}{dt} = k_m O_p - k_{-m} M \tag{32}$$

$$\frac{dA}{dt} = k_{ta} M - k_{-a} A - \alpha A T + \alpha_- C_1 \tag{33}$$

$$\frac{dT}{dt} = k_{ta} M - k_{-t} T - \alpha A T + \alpha_- C_1 - \beta C_1 T + \beta_- C_2 \tag{34}$$

$$\frac{dC_1}{dt} = \alpha A T - \alpha_- C_1 - \beta C_1 T + \beta_- C_2 \tag{35}$$

$$\frac{dC_2}{dt} = \beta C_1 T - \beta_- C_2, \tag{36}$$

where all variables retain their meaning from the basic RelBE model, and the new term is outlined by a dashed box.

Claim 6 The modification of the basic RelBE model described by Eqs. (31)–(36) cannot exhibit bistability in toxin concentration.

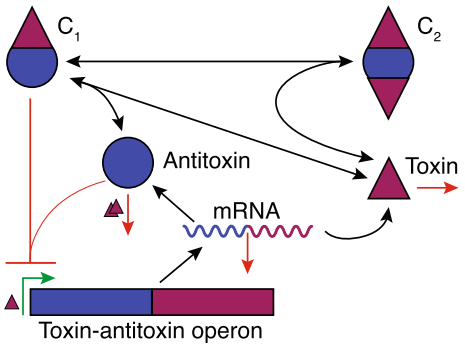

Fig. 7 Reaction diagram for the combination of mechanisms model. The model includes two operon states (ON and OFF); mRNA; antitoxin; toxin; and two complexes, C_1 and C_2. The operon is pictured in blue and maroon, representing the antitoxin and toxin gene, respectively. When the operon is derepressed, transcription of both antitoxin and toxin mRNA occurs, which are then translated into the two active protein forms. The active protein form of the antitoxin and toxin are represented by the blue circle and the maroon triangle, respectively. In this model, mRNA, the toxin protein, and the antitoxin protein are assumed to degrade. The first complex, C_1, is comprised of an antitoxin and toxin protein. We assume that C_1 can dissociate, repress the operon, but does not degrade. C_2, the second complex, is formed through the association of C_1 and an additional toxin monomer. C_2 has no role in operon repression, is assumed to dissociate, but not degrade. In the reaction diagram, black arrows represent physical transitions, and red arrows represent degradation or operon repression. This model combined toxin-mediated degradation of the antitoxin, antitoxin-mediated operon repression, and toxin-mediated operon derepression (color figure online)

Proof The steady-state equations for the system (31)–(36) can be reduced to a single cubic polynomial equation in T, which has the form:

$$n_1(T) = s_3T^3 + s_2T^2 + s_1T - s_0 = 0.$$

We can use the same argument as in Sect. 2.1 to show conclusively that this model cannot exhibit bistability in toxin concentration for any positive parameter regime. The same argument holds for the model in which the second complex represses the operon in coordination with the first complex. □

2.4 A few examples of bistable models

2.4.1 Combination of mechanisms model

Adding select combinations of mechanisms to the original RelBE model results in switch-like bistability. As an example, we consider the case when toxin-dependent activation of the operon, quadratic toxin-mediated degradation of the antitoxin, and additional antitoxin repression of the operon are added to the basic RelBE model. Figure 7 is the reaction diagram for this model. All assumptions from the original RelBE model carry over. The dimensional differential equation model has the follow-

ing representation:

$$\frac{dO_p}{dt} = kT(1-O_p) - k_- C_1 O_p - k_{-_2} A O_p \tag{37}$$

$$\frac{dM}{dt} = k_m O_p - k_{-m} M \tag{38}$$

$$\frac{dA}{dt} = k_{ta} M - k_{-a} A - \alpha A T + \alpha_- C_1 - k_s A T^2 \tag{39}$$

$$\frac{dT}{dt} = k_{ta} M - k_{-t} T - \alpha A T + \alpha_- C_1 - \beta C_1 T + \beta_- C_2 \tag{40}$$

$$\frac{dC_1}{dt} = \alpha A T - \alpha_- C_1 - \beta C_1 T + \beta_- C_2 \tag{41}$$

$$\frac{dC_2}{dt} = \beta C_1 T - \beta_- C_2, \tag{42}$$

where all variables retain their meaning from the basic RelBE model. The dimensional differential equation model can be nondimensionalized as follows:

$$\frac{dO_p}{d\tau} = p_1 t(1-O_p) - p_2 c_1 O_p - p_3 a O_p \tag{43}$$

$$\frac{dm}{d\tau} = p_4(O_p - m) \tag{44}$$

$$\frac{da}{d\tau} = p_4 m - p_5 a - p_6(at - c_1) - p_7 a t^2 \tag{45}$$

$$\frac{dt}{d\tau} = p_4 m - t - p_6(at - c_1) - p_8(c_1 t - c_2) \tag{46}$$

$$\frac{dc_1}{d\tau} = p_9(at - c_1) - p_{10}(c_1 t - c_2) \tag{47}$$

$$\frac{dc_2}{d\tau} = p_{11}(c_1 t - c_2), \tag{48}$$

where τ represents nondimensionalized time, O_p represents the probability the operon is in the ON state, and m, a, t, c_1, c_2 represent nondimensionalized concentrations

Table 1 Combination of mechanisms model nondimensionalized parameter denitions

Nondimensional parameter	Dimensional representation	Numerical value
p_1	$\frac{kk_{ta}k_m}{k_{-t}k_{-m}^2}$	0.02
p_2	$\frac{k_-\alpha k_{ta}^2 k_m^2}{k_{-t}k_{-m}^4\alpha_-}$	0.3
p_3	$\frac{k_{-2}k_{ta}k_m}{k_{-t}k_{-m}^2}$	1
p_4	$\frac{k_{-m}}{k_{-t}}$	20
p_5	$\frac{k_{-a}}{k_{-t}}$	2
p_6	$\frac{k_{ta}k_m\alpha}{k_{-m}^2k_{-t}}$	1
p_7	$\frac{k_{ta}^2k_m^2k_s}{k_{-m}^4k_{-t}}$	Bifurcation parameter
p_8	$\frac{k_{ta}^2k_m^2\beta\alpha}{k_{-m}^4k_{-t}\alpha_-}$	0.1
p_9	$\frac{\alpha_-}{k_{-t}}$	10
p_{10}	$\frac{k_{ta}k_m\beta}{k_{-m}^2k_{-t}}$	1
p_{11}	$\frac{\beta_-}{k_{-t}}$	1

of mRNA, antitoxin, toxin, the first complex, and the second complex, respectively. Parameters p_1-p_{11} are dimensionless parameters, which are defined in terms of the dimensional parameters in Table 1. The parameter p_7 is of particular interest as it controls quadratic toxin-mediated antitoxin degradation. The parameter p_7 can be thought about as encoding information about the level of stress of the cell's local environment.

For a select parameter regime (shown in Table 1), the system displays switch-like behavior in toxin concentration as a function of p_7, the parameter of interest. Figure 8 shows toxin bistability as a function of p_7. Figure 9 shows antitoxin bistability as a function of p_7.

In Fig. 10, p_1-p_7 space is explored through a two-parameter bifurcation diagram. A cusp bifurcation splits p_1-p_7 space into two regions. In region I, one antitoxin and toxin solution exists, whereas in region II, three toxin and antitoxin solutions exist. When p_1 is below the cusp point at $p_1 = 0.03$, bistability in the parameter p_7 occurs, as depicted in Figs. 8 and 9, whereas when p_1 is above the cusp point, bistability in p_7 is lost. Graded responses in toxin and antitoxin concentrations when $p_4 = 0.04$ are shown in Figs. 11 and 12, respectively.

In Fig. 13, a cusp bifurcation is shown in p_3-p_7 space, separating the space into two regions as in p_1-p_7 space. With p_3 below the cusp point, bistable behavior in p_7 is lost. Graded responses in toxin and antitoxin concentrations as a function of p_7 when $p_3 = 0.5$ are shown in Figs. 14 and 15, respectively. However, increasing p_3 creates a more dramatic switch. Figures 16 and 17 show switch-like behavior in toxin

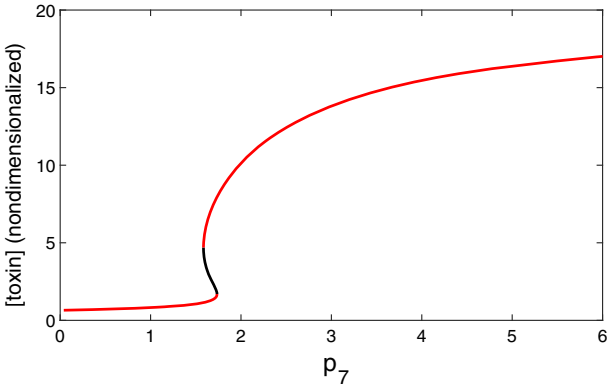

Fig. 8 Switch-like bistability in nondimensional toxin concentration as a function of p_7 for the parameter values $p_1 = 0.02$, $p_2 = 0.3$, $p_3 = 1$, $p_4 = 20$, $p_5 = 2$, $p_6 = 1$, $p_8 = 0.1$, $p_9 = 10$, $p_{10} = 1$, and $p_{11} = 1$ for the combination of mechanisms model (43)–(48)

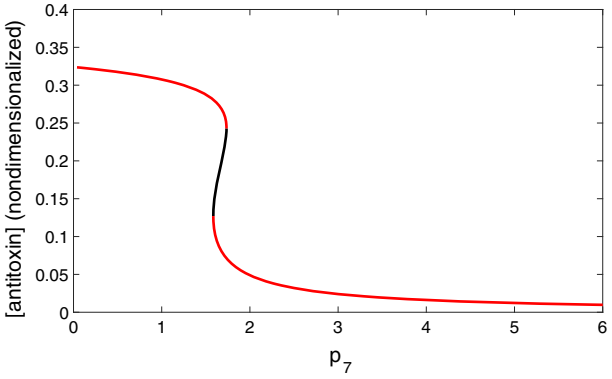

Fig. 9 Switch-like bistability in nondimensional antitoxin concentration as a function of p_7 for the parameter values $p_1 = 0.02$, $p_2 = 0.3$, $p_3 = 1$, $p_4 = 20$, $p_5 = 2$, $p_6 = 1$, $p_8 = 0.1$, $p_9 = 10$, $p_{10} = 1$, and $p_{11} = 1$ for the combination of mechanisms model (43)–(48)

and antitoxin concentrations, respectively, with a wider unstable range. Additional two parameter bifurcation diagrams are included in the Appendix.

2.4.2 A coupled TA model

It can be shown using the techniques we outlined that the basic RelBE model with the addition of toxin-dependent activation of the operon and antitoxin-dependent repression of the operon cannot exhibit bistability. However, pairing two systems of this type together with cross-toxin-mediated degradation of the sister antitoxin allows bistability to emerge. Others have also modeled cross interactions between TA systems (see Fasani and Savageau 2015). Figure 18 is the reaction diagram for this model. All assumptions from the original RelBE model carry over. The dimensional differential equation model has the following representation:

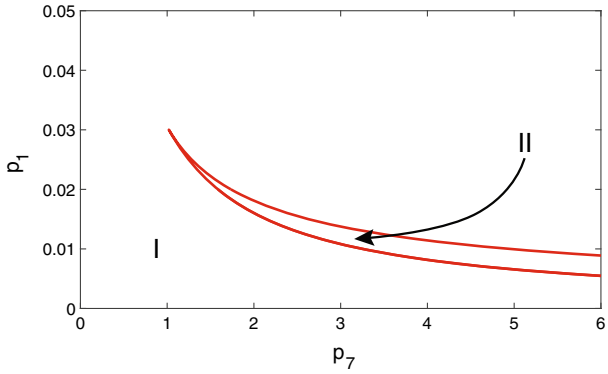

Fig. 10 Two parameter bifurcation plot in $p_7 - p_1$ space for the parameter values $p_2 = 0.3$, $p_3 = 1$, $p_4 = 20$, $p_5 = 2$, $p_6 = 1$, $p_8 = 0.1$, $p_9 = 10$, $p_{10} = 1$, and $p_{11} = 1$ for the combination of mechanisms model (43)–(48)

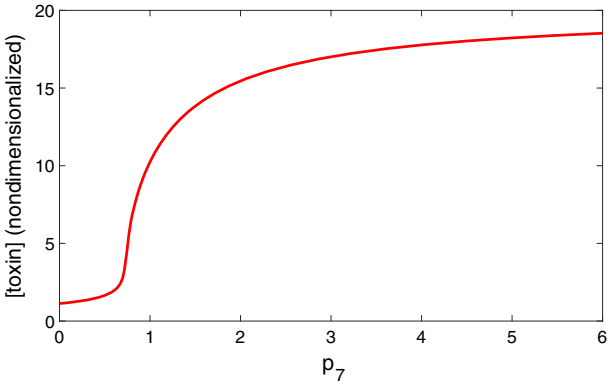

Fig. 11 Graded response in nondimensional toxin concentration as a function of p_7 for the parameter values $p_1 = 0.04$, $p_2 = 0.3$, $p_3 = 1$, $p_4 = 20$, $p_5 = 2$, $p_6 = 1$, $p_8 = 0.1$, $p_9 = 10$, $p_{10} = 1$, and $p_{11} = 1$ for the combination of mechanisms model (43)–(48)

$$\frac{dO_p}{dt} = kT(1 - O_p) - k_- C_1 O_p - k_{-_2} A O_p \tag{49}$$

$$\frac{dM_p}{dt} = k_m O_p - k_{-m} M_p \tag{50}$$

$$\frac{dA}{dt} = k_{ta} M_p - k_{-a} A - \alpha A T + \alpha_- C_1 \boxed{-k_{s_1} A X^2} \tag{51}$$

$$\frac{dT}{dt} = k_{ta} M_p - k_{-t} T - \alpha A T + \alpha_- C_1 - \beta C_1 T + \beta_- C_2 \tag{52}$$

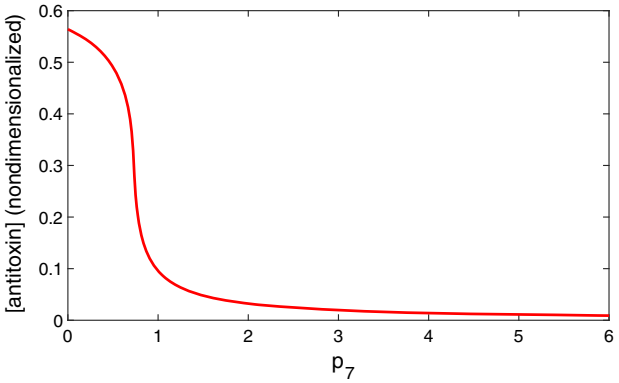

Fig. 12 Graded response in nondimensional antitoxin concentration as a function of p_7 for the parameter values $p_1 = 0.04$, $p_2 = 0.3$, $p_3 = 1$, $p_4 = 20$, $p_5 = 2$, $p_6 = 1$, $p_8 = 0.1$, $p_9 = 10$, $p_{10} = 1$, and $p_{11} = 1$ for the combination of mechanisms model (43)–(48)

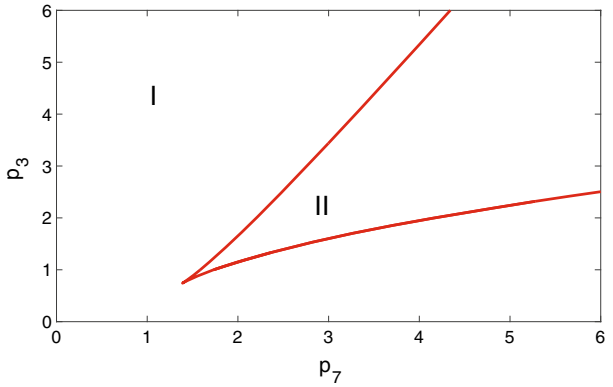

Fig. 13 Two parameter bifurcation plot in $p_7 - p_3$ space for the parameter values $p_1 = 0.02$, $p_2 = 0.3$, $p_4 = 20$, $p_5 = 2$, $p_6 = 1$, $p_8 = 0.1$, $p_9 = 10$, $p_{10} = 1$, and $p_{11} = 1$ for the combination of mechanisms model (43)–(48)

$$\frac{dC_1}{dt} = \alpha AT - \alpha_- C_1 - \beta C_1 T + \beta_- C_2 \tag{53}$$

$$\frac{dC_2}{dt} = \beta C_1 T - \beta_- C_2 \tag{54}$$

$$\frac{dO_s}{dt} = kX(1 - O_s) - k_- C_3 O_s - k_{-_2} W O_s \tag{55}$$

$$\frac{dM_s}{dt} = k_m O_s - k_{-m} M_s \tag{56}$$

$$\frac{dW}{dt} = k_{wx} M_s - k_{-w} W - \alpha W X + \alpha_- C_3 \boxed{-k_{s_2} W T^2} \tag{57}$$

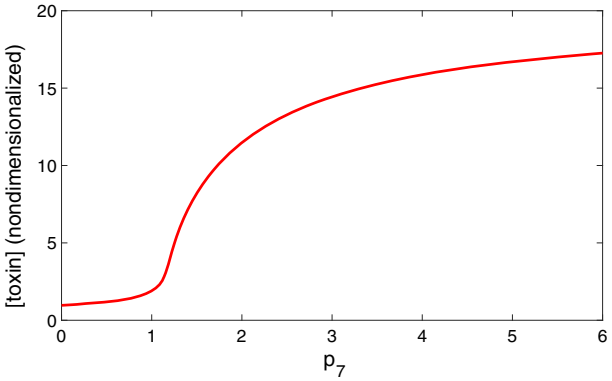

Fig. 14 Graded response in nondimensional toxin concentration as a function of p_7 for the parameter values $p_1 = 0.02$, $p_2 = 0.3$, $p_3 = 0.5$, $p_4 = 20$, $p_5 = 2$, $p_6 = 1$, $p_8 = 0.1$, $p_9 = 10$, $p_{10} = 1$, and $p_{11} = 1$ for the combination of mechanisms model (43)–(48)

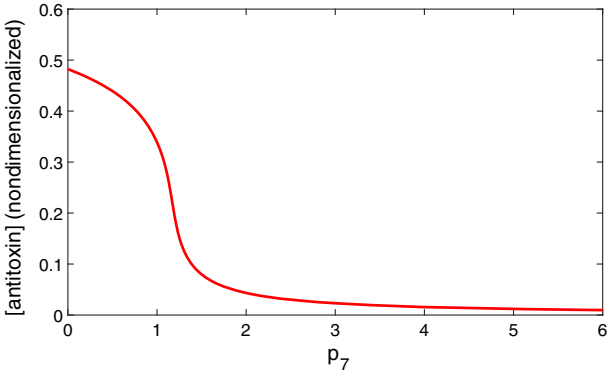

Fig. 15 Graded response in nondimensional antitoxin concentration as a function of p_7 for the parameter values $p_1 = 0.02$, $p_2 = 0.3$, $p_3 = 0.5$, $p_4 = 20$, $p_5 = 2$, $p_6 = 1$, $p_8 = 0.1$, $p_9 = 10$, $p_{10} = 1$, and $p_{11} = 1$ for the combination of mechanisms model (43)–(48)

$$\frac{dX}{dt} = k_{wx} M_s - k_{-x} X - \alpha W X + \alpha_- C_3 - \beta C_3 X + \beta_- C_4 \tag{58}$$

$$\frac{dC_3}{dt} = \alpha W X - \alpha_- C_3 - \beta C_3 X + \beta_- C_4 \tag{59}$$

$$\frac{dC_4}{dt} = \beta C_3 X - \beta_- C_4, \tag{60}$$

where the variables O_p, A, T, C_1, and C_2 retain their meaning from the basic RelBE model. The variable M_p has the same meaning as M in the basic RelBE model. O_s represents the probability a second TA operon is in the ON state, and M_s, W, X, C_3, C_4 represent concentrations of mRNA from the second type II TA system, a second antitoxin, a second toxin, the third complex, and the fourth complex, respectively. If

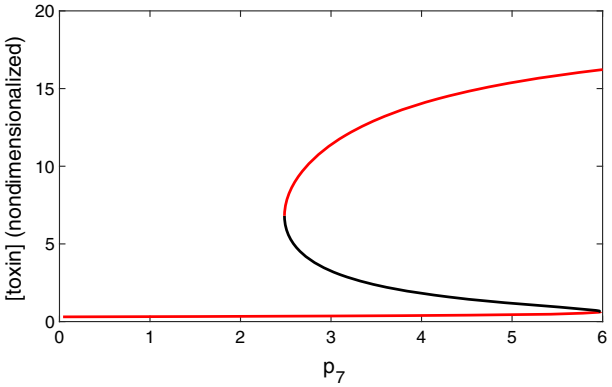

Fig. 16 Increasing p_3 creates a more dramatic switch in nondimensional toxin concentration as a function of p_7. The more dramatic switch exists for the parameter values $p_1 = 0.02$, $p_2 = 0.3$, $p_3 = 2.5$, $p_4 = 20$, $p_5 = 2$, $p_6 = 1$, $p_8 = 0.1$, $p_9 = 10$, $p_{10} = 1$, and $p_{11} = 1$ for the combination of mechanisms model (43)–(48)

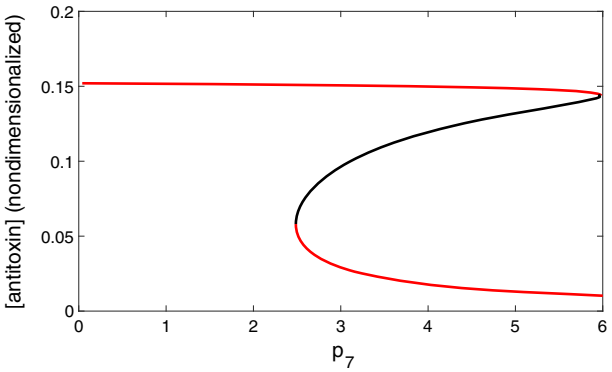

Fig. 17 Increasing p_3 creates a more dramatic switch in nondimensional antitoxin concentration as a function of p_7. The more dramatic switch exists for the parameter values $p_1 = 0.02$, $p_2 = 0.3$, $p_3 = 2.5$, $p_4 = 20$, $p_5 = 2$, $p_6 = 1$, $p_8 = 0.1$, $p_9 = 10$, $p_{10} = 1$, and $p_{11} = 1$ for the combination of mechanisms model (43)–(48)

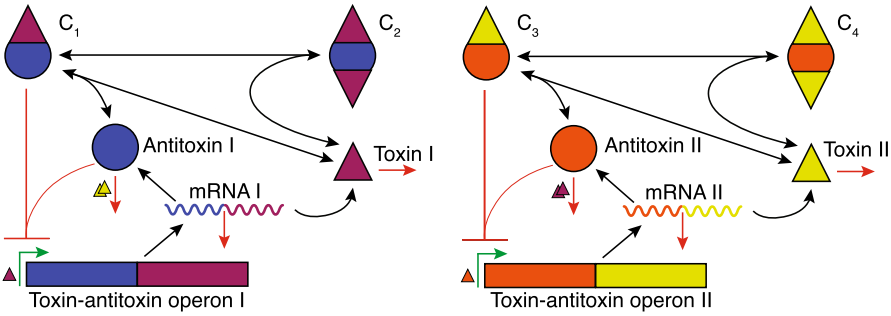

Fig. 18 Reaction diagram for the coupled TA model. This model gives an example of how two type II TA systems that in isolation would exhibit a graded response can exhibit bistable switch-like behavior when paired together. In this example, the mechanism is cross-toxin-mediated antitoxin degradation

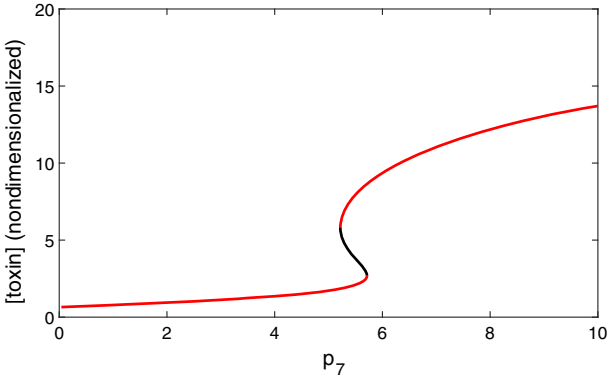

Fig. 19 Switch-like bistability in nondimensional first toxin concentration as a function of p_7 for the parameter values $p_1 = 0.02$, $p_2 = 0.3$, $p_3 = 1$, $p_4 = 20$, $p_5 = 2$, $p_6 = 1$, $p_8 = 0.1$, $p_9 = 10$, $p_{10} = 1$, $p_{11} = 1$, and $p_{12} = 0.5$ in the coupled TA model

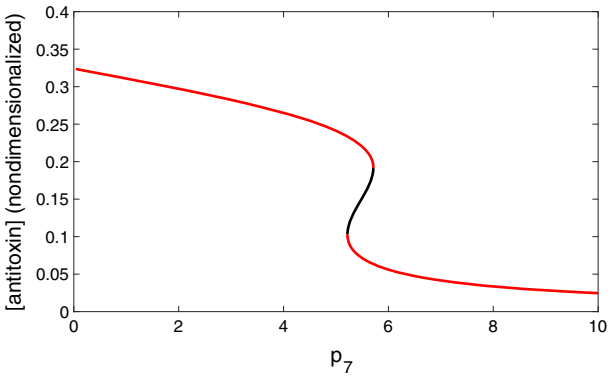

Fig. 20 Switch-like bistability in nondimensional first antitoxin concentration as a function of p_7 for the parameter values $p_1 = 0.02$, $p_2 = 0.3$, $p_3 = 1$, $p_4 = 20$, $p_5 = 2$, $p_6 = 1$, $p_8 = 0.1$, $p_9 = 10$, $p_{10} = 1$, $p_{11} = 1$, and $p_{12} = 0.5$ in the coupled TA model

k_{ta}=k_{wx}, k_{-a}=k_{-w}, and k_{-t}=k_{-x}, the dimensional differential equation model can be nondimensionalized as follows (assuming an analogous scaling for M_s, W, X, C_3, and C_4):

$$\frac{dO_p}{d\tau} = p_1 t(1 - O_p) - p_2 c_1 O_p - p_3 a O_p \tag{61}$$

$$\frac{dm_p}{d\tau} = p_4(O_p - m_p) \tag{62}$$

$$\frac{da}{d\tau} = p_4 m_p - p_5 a - p_6(at - c_1) - p_7 a x^2 \tag{63}$$

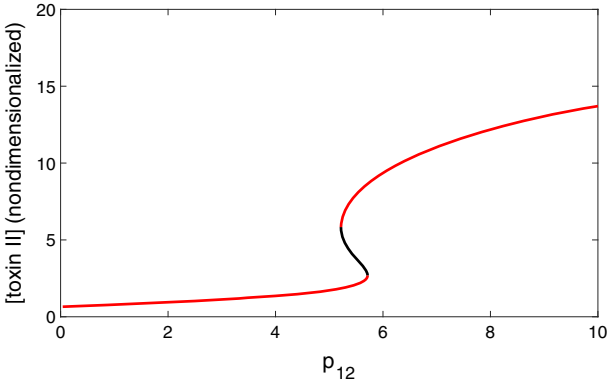

Fig. 21 Switch-like bistability in nondimensional second toxin concentration as a function of p_{12} for the parameter values $p_1 = 0.02$, $p_2 = 0.3$, $p_3 = 1$, $p_4 = 20$, $p_5 = 2$, $p_6 = 1$, $p_7 = 0.5$, $p_8 = 0.1$, $p_9 = 10$, $p_{10} = 1$, and $p_{11} = 1$ in the coupled TA model

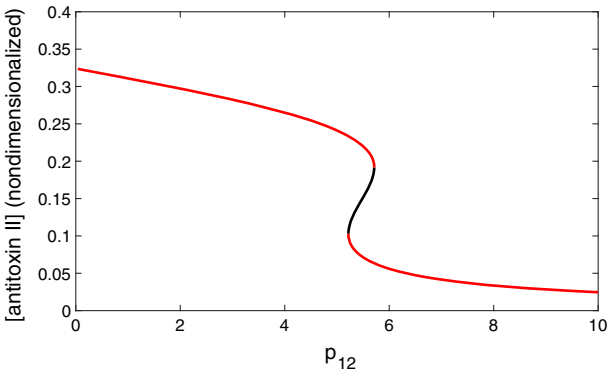

Fig. 22 Switch-like bistability in nondimensional second antitoxin concentration as a function of p_{12} for the parameter values $p_1 = 0.02$, $p_2 = 0.3$, $p_3 = 1$, $p_4 = 20$, $p_5 = 2$, $p_6 = 1$, $p_7 = 0.5$, $p_8 = 0.1$, $p_9 = 10$, $p_{10} = 1$, and $p_{11} = 1$ in the coupled TA model

$$\frac{dt}{d\tau} = p_4 m_p - t - p_6(at - c_1) - p_8(c_1 t - c_2) \tag{64}$$

$$\frac{dc_1}{d\tau} = p_9(at - c_1) - p_{10}(c_1 t - c_2) \tag{65}$$

$$\frac{dc_2}{d\tau} = p_{11}\,(c_1 t - c_2) \tag{66}$$

$$\frac{dO_s}{d\tau} = p_1 x(1 - O_s) - p_2 c_3 O_s - p_3 w O_s \tag{67}$$

$$\frac{dm_s}{d\tau} = p_4(O_s - m_s) \tag{68}$$

$$\frac{dw}{d\tau} = p_4 m_s - p_5 w - p_6(wx - c_3) - p_{12} w t^2 \tag{69}$$

$$\frac{dx}{d\tau} = p_4 m_s - x - p_6(wx - c_3) - p_8(c_3 x - c_4) \tag{70}$$

$$\frac{dc_3}{d\tau} = p_9(wx - c_3) - p_{10}(c_3 x - c_4) \tag{71}$$

$$\frac{dc_4}{d\tau} = p_{11}\,(c_3 x - c_4)\,, \tag{72}$$

where τ represents nondimensionalized time, O_p represents the probability the operon is in the ON state, and m_p, a, t, c_1, c_2 represent nondimensionalized concentrations of mRNA, antitoxin, toxin, the first complex, and the second complex, respectively. Similarly, O_p represents the probability the second TA operon is in the ON state, and m_s, w, x, c_3, c_4 represent nondimensionalized concentrations of the mRNA of the second type II TA system, a second antitoxin, a second toxin, the third complex, and the fourth complex, respectively. Parameters $p_1 - p_{12}$ are dimensionless parameters.

For a select parameter regime (shown in Table 1 and choosing $p_{12} = 0.5$), the coupled TA system displays switch-like behavior in toxin concentration as a function of p_7. Figure 19 shows toxin bistability as a function of p_7. Figure 20 shows antitoxin bistability as a function of p_7. Similarly, if p_{12} is chosen as the bifurcation parameter and $p_7 = 0.5$, bistability can be observed in the second toxin, X, and the second antitoxin W, as shown in Figs. 21 and 22, respectively.

3 Discussion

We began our search for bistability using a relatively simple model for the RelBE system. Using Descartes' rule of signs, we were able to show that the model could not display bistability for any possible combination of positive parameters. We then systematically added one additional mechanism to the RelBE model to study the emergence of bistability in type II TA systems. We consider many different mechanisms, some inspired by other biological systems, including complex, toxin, or antitoxin-mediated degradation of mRNA; decoupled translation rates; toxin-dependent degradation of the antitoxin; toxin-dependent operon activation; additional operon repression; and a combination of different mechanisms.

We found that adding any one of the mechanisms considered in this paper to the basic RelBE model never resulted in a model capable of instability. We used Descartes' rule of signs to prove the basic RelBE model with antitoxin-, toxin-, or complex mediated degradation of mRNA could not be bistable. We then considered the RelBE model with uncoupled translation rates. Again, in this case, we used Descartes' rule of signs to show that bistability could not occur for any combination of positive model parameters. When evaluating the possibility of bistability in the RelBE model with

toxin-dependent degradation of the antitoxin, we used a combination of Descartes' rule of signs and resultant analysis, specifically to search for double root transitions, to rule out switch-like and bistable behavior. Next, we modified the RelBE model with toxin-dependent activation of the operon, and we were able to prove that the system cannot exhibit sp bistablilty. To eliminate the possibility that bistability stemmed from additional operon repression, we modified the RelBE model to include additional repression from the antitoxin and the second complex. Again, we were able to show that in both cases the system could not exhibit bistability.

These findings are somewhat surprising, especially in the model for which there was toxin-dependent activation of the operon. The result that adding toxin-dependent activation of the operon to the basic RelBE model had no effect on sp bistabilty was surprising because of the similarity of the modified system to the SOS response, in which LexA represses DNA damage response genes then is cleaved off of the promoter site by single-stranded DNA-bound RecA. For a recent mathematical analysis of the SOS response, see FitzGerald and Keener (2021).

In our analysis, bistability emerged when multiple mechanisms were added to the RelBE model. Our "combination of mechanisms" model included several modifications to the original RelBE model. In particular, we added toxin-dependent derepression of the operon, quadratic toxin-mediated degradation of the antitoxin, and antitoxin-dependent repression of the operon. For a select parameter regime (shown in Table 1), the system displays switch-like behavior in toxin concentration as a function of p_7, the parameter of interest. Figure 8 shows toxin bistability as a function of p_7. Figure 9 shows antitoxin bistability as a function of p_7. None of the mechanisms listed above are sufficient as a singular addition to the basic RelBE to induce bistability in toxin concentration. It can also be shown using the techniques outlined in Sects. 2.1 and 2.3.3 that adding any two of the three above mechanisms is also insufficient to induce bistability. All three mechanisms that were added to the model are necessary for the emergence of bistability. However, it should be noted that the timescales of biological processes are not taken into account in the steady state and bifurcation analyses presented here.

We chose to use p_7 as our bifurcation parameter and explore the effect of p_1 and p_3 on bistability. In the case of p_1, the parameter controlling the toxin-dependent derepression of the operon, we found a narrow window for which bistable behavior occurs in p_1-p_7 space. In p_1-p_7 space, p_1 must be chosen to lie below the cusp point in Fig. 10. Choosing p_1 above the cusp point in Fig. 10 leads to a loss of bistable behavior, which is shown in Figs. 11 and 12. This result argues that for bistability to occur, the toxin must derepress the operon at a low level. We also found that p_3 controls the qualitative behavior of the switch. When we choose $p_3 = 1$ with all other parameters as in Table 1, we see a narrow switch region (see Figs. 8, 9), but when we increase p_3 to 2.5, there is a much more dramatic switch (shown in Figs. 16, 17). However, choosing p_3 too small also leads to a loss of bistable behavior, which is seen in Figs. 14 and 15.

Bistability also emerges by linking two identical type II TA system models that did not exhibit bistability in isolation with synergistic interactions. Our "coupled TA model" paired two RelBE models modified by the addition of toxin-dependent activation of the operon and antitoxin-dependent repression of the operon through

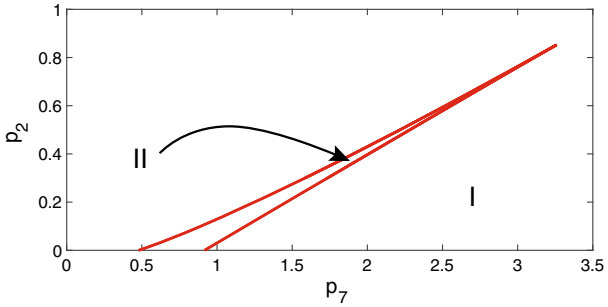

Fig. 23 Two parameter bifurcation plot in $p_7 - p_2$ space for the parameter values $p_1 = 0.02$, $p_3 = 1$, $p_4 = 20$, $p_5 = 2$, $p_6 = 1$, $p_8 = 0.1$, $p_9 = 10$, $p_{10} = 1$, and $p_{11} = 1$ in the combination of mechanisms model (43)–(48)

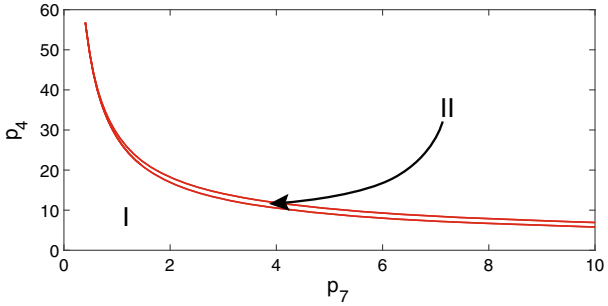

Fig. 24 Two parameter bifurcation plot in $p_7 - p_4$ space for the parameter regime $p_1 = 0.02$, $p_2 = 0.3$, $p_3 = 1$, $p_5 = 2$, $p_6 = 1$, $p_8 = 0.1$, $p_9 = 10$, $p_{10} = 1$, and $p_{11} = 1$ in the combination of mechanisms model (43)–(48)

cross-toxin-mediated degradation of the sister antitoxin. For a select parameter regime (shown in Table 1 and choosing $p_{12} = 0.5$), the coupled TA system displays switch-like behavior in toxin concentration as a function of p_7. Figure 19 shows toxin bistability as a function of p_7. Figure 20 shows antitoxin bistability as a function of p_7. Similarly, if p_{12} is chosen as the bifurcation parameter and $p_7 = 0.5$, bistability results in the second toxin, X, and the second antitoxin, W, which is shown in Figs. 21 and 22, respectively. In Figs. 23, 24, and 25 are shown two parameter bifurcation diagrams in $p_7 - p_2$, $p_7 - p_4$, and $p_7 - p_5$ parameter space, respectively. This simple result shows that cross-interactions or synergy between systems can drive the emergence of bistability and provides a mechanism (cross-toxin-mediated degradation of the sister antitoxin) by which this could occur.

Throughout our search for bistability, we relied on a combination of resultant analysis and Descartes' rule of signs, pairing these two disparate mathematical tools as a bistability indicator. This relatively simple technique definitively ruled out bistability as a possibility in many cases, which allowed us to avoid searching a high dimensional parameter space. In a previous modeling effort, Cataudella et al. could not definitively rule on bistability (Cataudella et al. 2013). Instead, Cataudella et al. relied on a numerical search to conclude that bistability was unlikely (Cataudella et al. 2013). It can

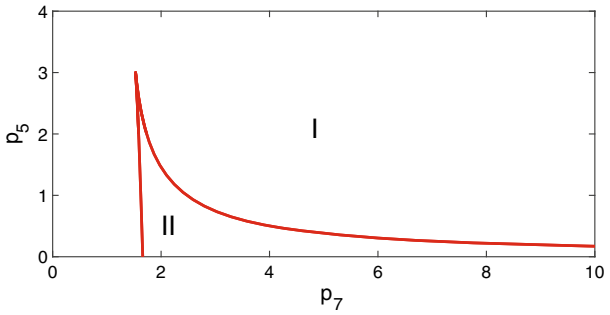

Fig. 25 Two parameter bifurcation plot in $p_7 - p_5$ space for the parameter regime $p_1 = 0.02$, $p_2 = 0.3$, $p_3 = 1$, $p_4 = 20$, $p_6 = 1$, $p_8 = 0.1$, $p_9 = 10$, $p_{10} = 1$, and $p_{11} = 1$ in the combination of mechanisms model (43)–(48)

be shown that the model in question cannot exhibit bistability for any combination of model parameters. Lou, Li, and Ouyang previously used a monotonicity argument to rule out bistability (Lou et al. 2008). Our analysis of type II TA systems demonstrates how Descartes' rule of signs and resultant analysis can be used together as a powerful tool in the search for bistable behavior across many mathematical systems, as well as providing deeper insights into how type II TA systems operate.

4 Conclusion

Our systematic search for bistability in type II TA systems identifies a new mechanistic explanation for how type II TA systems could exhibit bistability involving toxin-dependent operon derepression and shows how toxin bistability can result from synergistic interactions between paired type II TA systems. This study also demonstrated how Descartes' rule of signs and resultant analysis can be used as a delineator in the search for bistable behavior across many mathematical systems.

Appendix

Consider a variant of the model presented in Sect. 2.3.1 in which mRNA is degraded by the first complex, C_1. The model has the following form:

$$\frac{dO_p}{dt} = k(1 - O_p) - k_- C_1 O_p \tag{73}$$

$$\frac{dM}{dt} = k_m O_p - k_{-m} M \boxed{-k_{-m_2} M C_1} \tag{74}$$

$$\frac{dA}{dt} = k_{ta} M - k_{-a} A - \alpha A T + \alpha_- C_1 \tag{75}$$

$$\frac{dT}{dt} = k_{ta}M - k_{-t}T - \alpha AT + \alpha_- C_1 - \beta C_1 T + \beta_- C_2 \tag{76}$$

$$\frac{dC_1}{dt} = \alpha AT - \alpha_- C_1 - \beta C_1 T + \beta_- C_2 \tag{77}$$

$$\frac{dC_2}{dt} = \beta C_1 T - \beta_- C_2, \tag{78}$$

The steady-state equations for the system (73)–(78) can be reduced to two polynomials equations in T and A, which we denote as $n_1(T, A)$ and $n_2(T, A)$. $n_1(T, A)$ has the following form:

$$\begin{aligned} n_1(T, A) = &-(T^2\alpha^2 k_{-a}k_{-}k_{-m_2})A^3 - (T\alpha k_{-a}\alpha_-)(kk_{-m_2} + k_-k_{-m})A^2 \\ &- (\alpha_-^2 kk_{-a}k_{-m})A + k\alpha_-^2 k_m k_{ta} = 0, \end{aligned}$$

and $n_2(T, A)$ has the form

$$\begin{aligned} n_2(T, A) = &(-T^3\alpha^2 k_-k_{-m_2}k_{-t})A^2 - (T^2\alpha k_{-t}\alpha_-)(kk_{-m_2} + k_-k_{-m})A \\ &- k\alpha_-^2(Tk_{-m}k_{-t} - k_m k_{ta}) = 0. \end{aligned}$$

The resultant of $n_1(T, A)$ and $n_2(T, A)$ with respect[2] to A is a polynomial in T with the form:

$$\begin{aligned} r_1(T) = &(\alpha^2 k_-k_{-m_2}k_{-t}^3)T^5 + \alpha k_{-a}k_{-t}^2\alpha_-(kk_{-m_2} + k_-k_{-m})T^3 \\ &+ (kk_{-a}^2 k_{-m}k_{-t}\alpha_-)T - kk_m k_{-a}^2 k_{ta}\alpha_-^2 = 0. \end{aligned}$$

Using a Descartes Rule of Signs argument, we can see that this model variant cannot exhibit bistable switch-like behavior for any positive parameter set.

A note on software

It should be noted that XPP AUTO was used to create the bifurcation diagrams presented in this paper We used Ting-Hao Hsu's Matlab interface for plotting the diagrams (available at math.pitt.edu/ bard/xpp/xpp.html).

References

Afif H, Allali N, Couturier M, Van Melderen L (2001) The ratio between CcdA and CcdB modulates the transcriptional repression of the ccd poison–antidote system. Mol Microbiol 41(1):73–82. https://doi.org/10.1046/j.1365-2958.2001.02492.x

Bukowski M, Rojowska A, Wladyka B (2011) Prokaryotic toxin–antitoxin systems—the role in bacterial physiology and application in molecular biology. Acta Biochim Pol 58(1):1–9

Cataudella I, Sneppen K, Gerdes K, Mitarai N (2013) Conditional cooperativity of toxin-antitoxin regulation can mediate bistability between growth and dormancy. PLoS Comput Biol 9(8):e1003174. https://doi.org/10.1371/journal.pcbi.1003174

[2] The entries of the Sylvester Matrix are the coefficients of the two polynomials. In this case, we have two polynomials in T and A, so we could build two different matrices from the coefficients of either A or T. The phrase "with respect to A" indicates that the entries of the Sylvester Matrix are based on the coefficients of A rather than T, and T is treated as a coefficient of the polynomial in A.

Fasani RA, Savageau MA (2015) Unrelated toxin–antitoxin systems cooperate to induce persistence. J R Soc Interface 12(108):20150130. https://doi.org/10.1098/rsif.2015.0130
FitzGerald CE, Keener JP (2021) The PafBC-mediated response sensitizes a bistable DNA damage response in Mycobacteria. J Theor Biol 508:110462. https://doi.org/10.1016/j.jtbi.2020.110462
Fraikin N, Rousseau CJ, Goeders N, Van Melderen L (2019) Reassessing the role of the type II MqsRA toxin–antitoxin system in stress response and biofilm formation: MqsA is transcriptionally uncoupled from mqsR. mBio 10(6):1–13. https://doi.org/10.1128/mBio.02678-19
Garcia-Pino A, Balasubramanian S, Wyns L, Gazit E, De Greve H, Magnuson RD, Charlier D, van Nuland NA, Loris R (2010) Allostery and intrinsic disorder mediate transcription regulation by conditional cooperativity. Cell 142(1):101–111. https://doi.org/10.1016/j.cell.2010.05.039
Germain E, Roghanian M, Gerdes K, Maisonneuve E (2019) Retraction: Stochastic induction of persister cells by HipA through (p)ppGpp-mediated activation of mRNA endonucleases (Proceedings of the National Academy of Sciences of the United States of America (2015) 112 (51715176) https://doi.org/10.1073/pnas.1423536112). Proc Natl Acad Sci USA 166(22):11077. https://doi.org/10.1073/pnas.1906160116
Goormaghtigh F, Fraikin N, Putrin M, Hallaert T, Hauryliuk V, Garcia-Pino A, Sjdin A, Kasvandik S, Udekwu K, Tenson T, Kaldalu N, Van Melderen L (2018) Reassessing the role of type II toxin–antitoxin systems in formation of *Escherichia coli* type II persister cells. mBio 9(3):1–14. https://doi.org/10.1128/mBio.00640-18
Graham TG, Tabei SM, Dinner AR, Rebay I (2010) Modeling bistable cell-fate choices in the Drosophila eye: qualitative and quantitative perspectives. Development 137(14):2265–2278. https://doi.org/10.1242/dev.044826
Harms A, Brodersen DE, Mitarai N, Gerdes K (2018) Toxins, targets, and triggers: an overview of toxin–antitoxin biology. Mol Cell 70(5):768–784. https://doi.org/10.1016/j.molcel.2018.01.003
Harms A, Fino C, Sørensen MA, Semsey S, Gerdes K (2017) Prophages and growth dynamics confound experimental results with antibiotic-tolerant persister cells. mBio 8(6):1–18. https://doi.org/10.1128/mBio.01964-17
Lou C, Li Z, Ouyang Q (2008) A molecular model for persister in *E. coli*. J Theor Biol 255(2):205–209
Maisonneuve E, Castro-camargo M, Gerdes K (2018a) Retraction Notice to: (p) ppGpp controls bacterial persistence by stochastic induction of toxin–antitoxin activity, vol 1. https://www.cell.com/abstract/S0092-8674(13)00958-6
Maisonneuve E, Shakespeare LJ, Girke M (2018b) Retraction: Bacterial persistence by RNA endonucleases (Proceedings of the National Academy of Sciences of the United States of America (2011) 108 (13206-13211 10.1073/pnas.1100186108) Proc Natl Acad Sci USA. 115:E2901. https://doi.org/10.1073/pnas.1803278115
Overgaard M, Borch J, Jørgensen MG, Gerdes K (2008) Messenger RNA interferase RelE controls relBE transcription by conditional cooperativity. Mol Microbiol 69(4):841–857. https://doi.org/10.1111/j.1365-2958.2008.06313.x
Puszyński K, Hat B, Lipniacki T (2008) Oscillations and bistability in the stochastic model of p53 regulation. J Theor Biol 254(2):452–465. https://doi.org/10.1016/j.jtbi.2008.05.039
Ramisetty BCM (2020) Regulation of type II toxin–antitoxin systems: the translation-responsive model. Front Microbiol 11:1–6. https://doi.org/10.3389/fmicb.2020.00895
Smolen P, Baxter DA, Byrne JH (2019) How can memories last for days, years, or a lifetime? Proposed mechanisms for maintaining synaptic potentiation and memory. Learn Mem 26:1–59. https://doi.org/10.1101/lm.049395.119.Freely
Unterholzner SJ, Poppenberger B, Rozhon W (2013) Toxin–antitoxin systems. Mob Genet Elem 3(5): https://doi.org/10.4161/mge.26219